[AMERICAN JOURNAL OF SCIENCE, VOL. 292, NOVEMBER, 1992, P. 659–683]

THE REACTIVITY OF SEDIMENTARY IRON MINERALS TOWARD SULFIDE

DONALD E. CANFIELD*, ROBERT RAISWELL**, and SIMON BOTTRELL**

ABSTRACT. Sediment from the FOAM (Friends of Anoxic Mud) site in Long Island Sound, Connecticut, was partitioned into several different size fractions (and magnetite), and the concentration and isotopic composition of sulfur in each fraction was determined. Size fractions were chosen to represent different associations of pyrite with iron. For example, pyrite in the 4 to 21 μm size fraction was mostly framboidal and the earliest formed; by contrast pyrite in the 21 to 63 μm size fraction was found to form later and only on and within the layers of sheet silicate minerals. Sulfur isotopes were found to reflect the various stages of pyrite formation, with later formed pyrites up to 40 permil heavier in ^{34}S than the earliest formed pyrites. Sulfur concentration data show that iron is reacted from sheet silicates (the largest pool of unpyritized iron at FOAM) with a half-life of about 100,000 yrs. Sheet silicates react with sulfide about 10^8 times more slowly than the most reactive iron oxyhydroxides in sediments. Such dramatic differences in reactivity explain why sulfide builds up in pore solution after iron oxides are consumed in pyrite formation. Lastly, these data demonstrate that calculated values of sediment DOP (degree of pyritization) cannot be used to demonstrate uniquely iron or sulfur limitation in pyrite formation. Rather, what limits pyrite formation will depend on the relative rates of sulfate reduction compared to rates of sulfide reaction with iron minerals; DOP does not yield information on these factors.

INTRODUCTION

The concentrations of solid-phase iron and its reactivity toward sulfide are among the important factors limiting the formation of pyrite in marine sediments (Berner, 1984; Raiswell and Berner, 1985). It is obvious that iron will limit pyrite formation when more sulfide is available for reaction with iron, than there is iron to react with. Iron limitation may be common in marine sediments, particularly those around the continental margins, where rates of sulfide formation often far exceed the burial rates of iron (Canfield and Raiswell, 1991). Most studies have determined iron limitation by comparing the amounts of iron present as the mineral pyrite, with the amounts liberated from a standardized acid digestion (Berner, 1970; Raiswell and Berner, 1985; Dean and Arthur, 1989). The iron liberated in acid is assumed to be potentially reactive toward sulfide, and the degree of pyritization of the sediment (DOP; Berner, 1970; Raiswell and Berner, 1985; Raiswell and others, 1988) is

* School of Earth and Atmospheric Sciences, Georgia Institute of Technology, Atlanta, Georgia 30332-0340
** Department of Earth Sciences, University of Leeds, Leeds LS2 9JT United Kingdom

given as:

$$\text{DOP} = \frac{\text{Fe(pyrite)}}{\text{Fe(pyrite)} + \text{Fe(acid-soluble)}} \quad (1)$$

Iron limitation is assumed to occur at high values of DOP (near to one, where little further potentially reactive iron is available). High DOP values are often associated with euxinic environments where sediment may have contacted sulfide for a considerable length of time. As such, DOP has proven to be a useful tool in distinguishing paleoenvironments (Raiswell and others, 1988). In modern sediment studies, however, relatively low DOP values (0.2–0.4, for example) may be measured in anoxic, sulfidic, sediments where the concentrations of pyrite sulfur are relatively constant with sediment depth (Berner, 1970; Jørgensen, 1978a), implying little reaction between sulfide and iron. Also, in some cases, it has been demonstrated that considerable amounts of sulfide do not react with iron and, instead, are lost from the sediment by diffusion and reoxidation (for example, Limfjorden in Denmark; Jørgensen, 1977). Whereas DOP values in these cases imply that pyrite is not iron-limited, it is clear that on early diagenetic time scales, much of the acid-soluble iron in the sediment is relatively unreactive toward sulfide.

These observations suggest that "iron limitation" is a relative term and depends on the rates with which sulfide reacts with iron minerals compared to the rates of sulfide production. In the present study we explore the reaction rates between dissolved sulfide and important iron-containing sedimentary phases, defined either directly by mineral separation or indirectly by chemical extractions. We constrain reaction rates both by determining pyrite sulfur formation rates with sediment depth and by analyzing the isotopic composition of sulfur associated with the different iron pools. These results constrain the reaction rates of different iron phases toward sulfide and show how the reactivity of iron toward sulfide can affect the isotopic composition of sedimentary sulfides.

METHODS

Sediment from the FOAM site in Long Island Sound, Connecticut, was used for this study (for a site description see Goldhaber and others, 1977; Aller, 1980a,b; Krishnaswami and others, 1984; Canfield, 1989). Sediment was obtained from both a diver collected box core as well as a 3 meter-long vibracore. The box core was constructed as described by Aller (ms). The vibracorer contained a plastic inner core liner placed inside the aluminum outer tube, so that the sediment was held within the plastic liner as the aluminum tube penetrated the sediment during coring. This eliminated any potential corrosive reactions between the metal outer tube and the sediment and allowed for visual inspection of the sediment. On recovery, the vibracore sediment looked remarkably undisturbed, and this was verified by a strong similarity between chemical profiles

obtained from the vibracore and profiles from shorter gravity cores. Both vibracore and box core sediment were sectioned and processed within a few hours of collection in a N_2-filled glove bag.

Sediment pore waters were obtained by centrifugation, and dissolved iron, sulfide and sulfate were analyzed as described in Canfield (1989). Pyrite sulfur was liberated by chromium reduction, and its concentration determined by iodometric titration (Canfield and others, 1986). Reduced sulfur for isotopic analysis was also liberated by chromium reduction and collected as Ag_2S. The Ag_2S was converted to SO_2 (Robinson and Kusakabe, 1975), and the isotope ratios of $^{34}S/^{32}S$ were measured with a VG Sira 10 gas source mass spectrometer. Pore water sulfide was collected at four depth intervals below 20 cm for isotopic analysis by acid distillation of frozen sediment. This method is not ideal because of potential contributions from acid volatile iron sulfides. Below about 20 cm depth, however, acid volatile iron sulfides are in very low concentration as demonstrated by the similar quantities of sulfide liberated by acid digestion, as compared to separate pore water sulfide determinations (see above). Hence, these data should at least approximate the isotopic composition of pore water sulfide with depth at FOAM. Organic and inorganic carbon concentrations were obtained as described by Krom and Berner (1983) using a LECO carbon analyzer. DOP values were determined at several levels in the vibracore sediment by boiling freeze-dried sediment for one minute in concentrated 12 N HCl and combining these data with pyrite-Fe contents (Berner, 1970; Raiswell and others, 1988).

The iron oxide content of the box core sediment was determined using the scheme described in Canfield (ms and 1989). Briefly, iron oxides were partitioned by an acidic oxalate solution into "easily extractable" phases (including ferrihydrite and lepidocrocite) and "more crystalline" oxides (representing hematite and goethite) calculated as the difference between the oxalate and a dithionite extraction. Acid volatile sulfides (AVS, mostly FeS) oxidize in air to an iron oxide phase removed by both extractions (Canfield, 1989), and its contribution to the oxide determinations was corrected with a separate AVS digestion on fresh, unoxidized sediment (Canfield, 1989).

Magnetite was removed from freeze-dried sediment using a strong magnet (Canfield and Berner, 1987), and the sulfur overgrowing the magnetites (see Canfield and Berner, 1987) was collected for isotopic analysis as described above. Both box core and vibracore sediment were partitioned at several depths into various size fractions. Size fractions of >63 μm and 21 to 63 μm were collected by wet sieving. Before sieving sediment was briefly sonicated (2–3 min) to dissaggregate any sediment clumps. The 4 to 21 μm fraction was separated from the <4 μm fraction by gravity settling a homogenized mixture of the two size fractions in distilled H_2O. Settling times were determined by Stokes law, and after settling was complete, water overlying the 4 to 21 μm fraction was removed (this contained the <4 μm fraction). The 4 to 21 μm fraction,

which at this point still contained some clay material, was rehomogenized, and settling was repeated (at least 4 times) until no further clay remained suspended when settling was complete.

These size fractions were chosen, as much as possible, to separate and collect pyrite which was uniquely associated with different iron phases (pyrite overgrown onto magnetite and sheet silicates for example; see below), with organic material (grown into forams or onto plant debris), or of a unique morphology (framboidal pyrite). Size fractions were thus chosen, by trial and error, to accomplish best these different separations. We stress that the size fractions used here were optimized for the conditions of pyritization found at FOAM; other sites may require a somewhat different separation of sizes. For example, we have observed that pyrite framboids from the Mississippi Delta may reach 50 μm in size and will not be separated with this same protocol.

For each size fraction, reduced sulfur was collected (as described above) for isotopic analysis, and its concentration determined. The total iron content of each size fraction was obtained using an HF/HNO_3 dissolution scheme as described by Canfield (1989), with final analysis by atomic absorption spectrometry (AAS). Scanning electron microscope (SEM) observations were made on graphite coated particles using an ETEC Autoscan, coupled with a Tracor Northern model 2000 energy dispersive spectrometer (EDS) for chemical analysis. Positive mineral identification at several depths for the different size fractions was made from X-ray diffraction powder patterns. Bulk chemical analysis by X-ray fluorescence (XRF) was performed for the different size fractions at a few selected depths.

RESULTS

Sediment chemistry.—The depth distributions of dissolved iron and sulfide, as well as the speciation of solid phase iron for the box core sediment, are shown in figure 1A (see also Canfield, 1989). The concentrations of dissolved sulfide and pyrite sulfur (on a carbonate-free basis) are shown in figure 1B for the vibracore sediment. The wt percent iron and reduced sulfur for the various size fractions are shown in figure 2. The >63 μm fraction contained mostly shelly carbonate with very little clastic mineral matter and will not be considered further (very little carbonate was passed into the smaller fractions). The isotopic compositions of sulfur for the various size fractions, the pyrite coated onto magnetite, the total sediment, and dissolved H_2S are shown in figure 3. Bulk sediment chemistry by X-ray fluorescence is shown in table 1, and HCl extractable iron, total iron, sulfur-bound iron, and DOP are given for several depth intervals in table 2.

Sediment mineralogy.—From XRD results, visual examination, and bulk sediment chemistry (table 1), the mineralogy of FOAM sediment is uniform with depth. The major mineral phase is quartz, and next in importance are feldspar and sheet silicates (mostly chlorite and muscovite). Other than the iron oxides near the sediment surface, chlorite is the

most abundant iron-containing mineral phase. Many other iron-containing phases are present including biotite, garnets, pyroxenes, amphiboles, and various spinels, all of which may be observed in heavy mineral separates and under the SEM but are too minor to show up in XRD powder patterns. The 4 to 21 μm and 21 to 63 μm size fractions are similar in their mineralogy and reflect the bulk sediment mineralogy as discussed above. The clay-size fraction (<4 μm) was depleted in quartz and feldspar relative to the other size fractions and enriched in the layered silicates as evidenced by prominent 14, 10, and 7 Å XRD peaks. Due to small particle size, however, the minerals in the clay fraction gave only weak X-ray reflections, and no attempt was made to characterize them further.

Pyrite in the different size fractions.—FOAM sediment was partitioned into various size fractions (and magnetite) in order to isolate pyrite formed during different stages of diagenesis from iron minerals with differing reactivity toward sulfide. Iron reactivity will be discussed below; here we will describe briefly the forms of pyrite in the different size fractions and the nature of their association with different iron-containing minerals.

In the 4 to 21 μm size fraction, individual pyrite framboids were the most abundant form of pyrite, and, in fact, most of the framboidal pyrite in the sediment occurred in this fraction. Pyrite framboids were extremely rare in the 21 to 63 μm size fraction, and virtually all the pyrite in this fraction was associated with sheet silicates (in both the 4–21 and 21–63 μm fractions a very small amount of the total pyrite was associated with plant debris). Chlorite was the most abundant iron-containing layered silicate (see p.), but some biotite was also observed under the SEM (as determined by significant concentrations of both Fe and K using EDS). Pyrite was observed forming on the surface of layered silicates (fig 4A) and also between silicate layers (fig 4B). This pyrite probably formed by the reaction between the iron contained within the silicate lattice and dissolved sulfide which reaches and sustains quite an appreciable concentration at FOAM (fig. 1B).

With the SEM, we also observed that some of the sheet silicates at the sediment surface contained large amounts of interlayer iron oxides. In backscatter these iron oxides appeared much the same as the interlayer pyrite farther down in the sediment. We suggest that the iron oxides are oxidized interlayer pyrite, and that some of the sheet silicates at FOAM have been through various episodes of pyritization and reoxidation, perhaps in salt marshes which line much of the coast. It is important, though, that sheet silicates may contain both iron oxides and silicate-iron for reaction with sulfide.

Pyrite in the clay size fraction was very fine grained, with some very small framboids present. Mostly, however, the pyrite was too small to observe, and the association between pyrite and iron minerals in the clay fraction is unknown. The association between pyrite and magnetite at FOAM was discussed previously (Canfield and Berner, 1987). Below

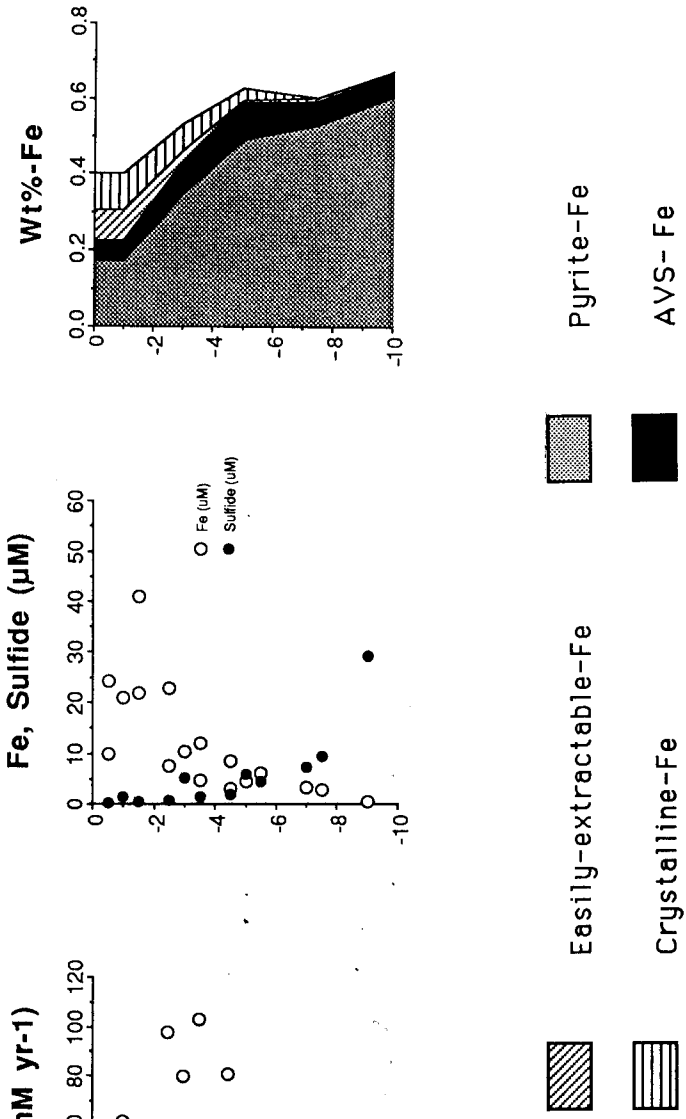

Fig. 1(A). The distribution of sulfate reduction rate (from Westrich, 1983), dissolved pore water iron and sulfide, and solid-phase iron speciation, are shown for the top 10 cm at FOAM.

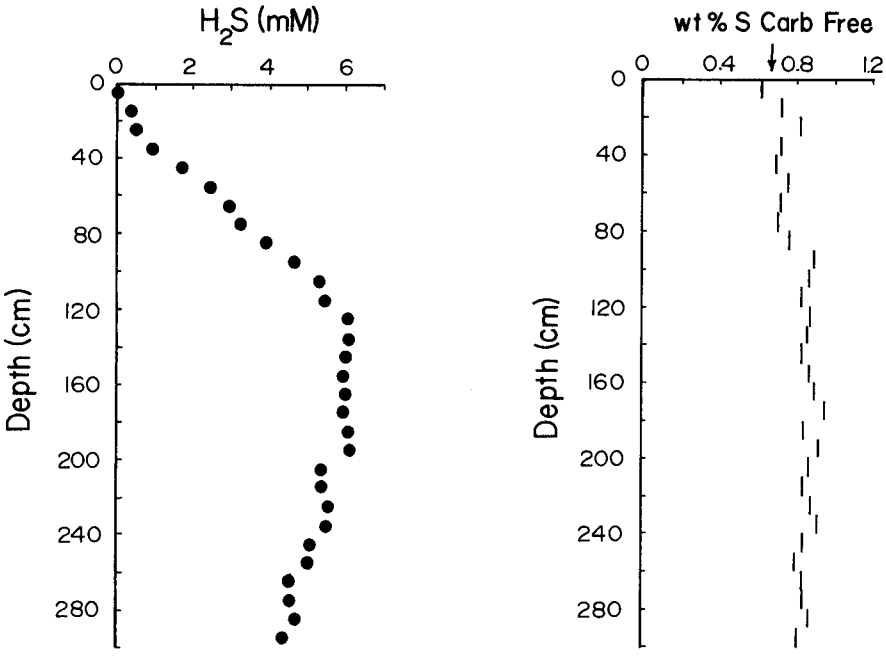

(B) Dissolved pore water sulfide and total reduced sulfur (carbonate free) are presented to 3 m depth at FOAM.

about 60 cm magnetite becomes completely overgrown by pyrite due to the reaction between dissolved sulfide and magnetite iron (fig. 4C). In the present study the concentrations of magnetite with sediment depth were not carefully quantified, but pyritized magnetite was found over the full 3 m depth of the vibracore.

DISCUSSION

Reaction rates between sulfide and iron.—We will begin with some general qualitative comments about reaction rates and then attempt to quantify some of these rates. From figure 1B, it is clear that pyrite forms early at FOAM, mostly within the top 10 cm of the sediment. With increasing sediment depth there is very little additional pyrite formation, despite high concentrations of dissolved sulfide. In the vibracore (and in general at FOAM) sulfate was depleted from the pore waters at about 150 cm (see also Goldhaber and others, 1977; Westrich, ms), with no more sulfate reduction possible below this depth. The very gradual decrease in dissolved sulfide below 150 cm (fig. 1B) further demonstrates the slow reaction between sulfide and iron minerals deep at FOAM, considering that each meter of sediment depth represents about 1000 yrs of deposition.

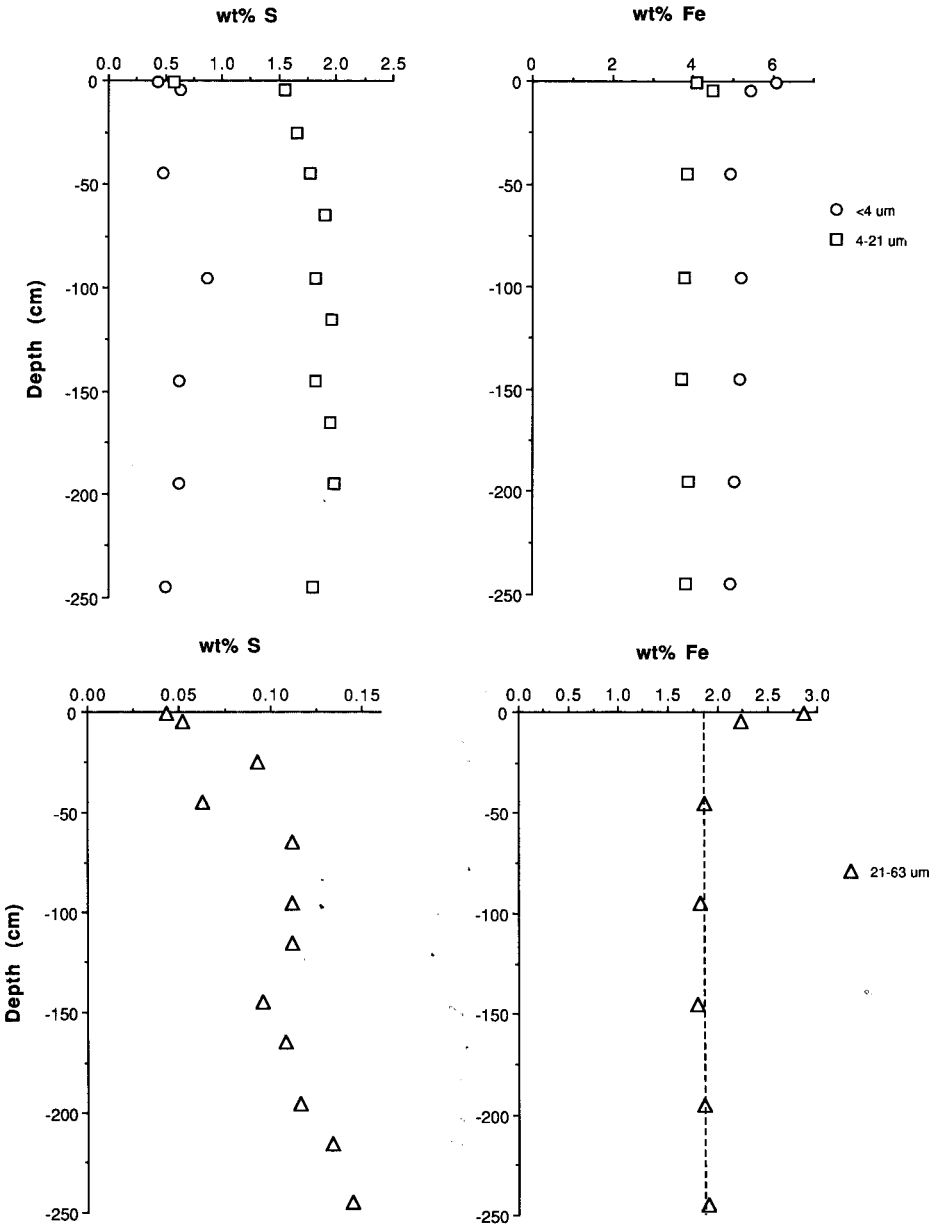

Fig. 2. Depth distributions of total reduced sulfur and total Fe are shown, with depth, for various size fractions. See text details on size separations.

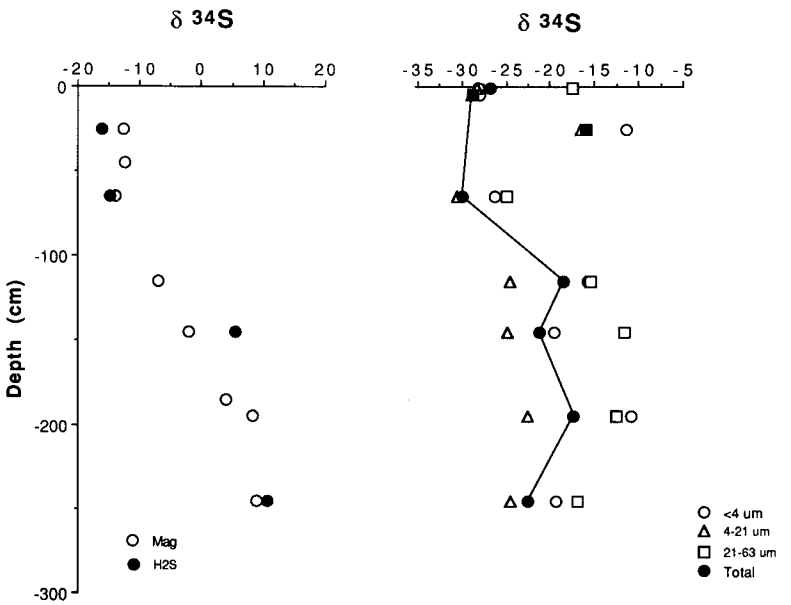

Fig. 3. $\delta^{34}S$ for reduced sulfur from the various size fractions, dissolved pore water sulfide, and pyrite overgrown onto magnetite. The solid line connects the total sulfur data. Results from the 20 to 30 depth interval are believed to reflect pyrite formation under non-steady state conditions (see text for details).

TABLE 1

Elemental analysis of size separates

	60–70		140–150	160–170			240–250	
Depth (cm)	Total	21–63 μm	Total	<4 μm	4–21 μm	21–63 μm	Total	21–63 μm
SiO_2	61.09	73.41	62.77	49.60	64.98	73.42	60.40	73.81
TiO_2	0.75	0.82	0.77	0.67	0.99	0.73	0.70	0.66
Al_2O_3	11.35	11.23	11.82	14.69	12.62	11.52	12.19	11.82
Fe_2O_3	4.26	2.89	4.37	7.11	5.57	2.84	4.72	2.84
MnO	0.08	0.08	0.09	0.11	0.15	0.07	0.09	0.06
MgO	1.59	1.02	1.64	2.67	1.35	1.05	1.77	1.02
CaO	7.26	3.35	5.90	2.29	2.22	3.00	5.91	2.47
Na_2O	2.48	2.57	2.58	2.94	2.35	2.00	2.33	2.49
K_2O	2.07	1.80	2.18	2.94	2.35	2.00	2.33	2.07
P_2O_5	0.14	0.18	0.15	0.16	0.16	0.15	0.14	0.14
L.O.I.	6.86	2.22	5.53	16.00	5.70	2.03	6.39	2.02
Total	97.92	99.71	97.81	97.03	98.30	99.33	97.18	99.45

TABLE 2
DOP with depth at FOAM

Depth (cm)	S-bound Fe	HCl-Fe	Total-Fe	DOP
10–20	0.711	0.962	3.06	0.425
60–70	0.627	0.905	2.72	0.409
140–150	0.718	0.901	3.16	0.443
190–200	0.774	1.190	3.35	0.394
250–260	0.628	0.932	2.91	0.403

The rapid formation of pyrite near the sediment surface at FOAM reflects the rapid reaction between sulfide and iron oxides (excluding magnetite). Evidence for this comes from field observations where, even with high rates of sulfate reduction, dissolved sulfide will not accumulate in sediment pore waters when iron oxides are present (Canfield, 1989; Canfield and Raiswell, 1991; fig. 1A). Also, experimental studies have confirmed that iron oxides may react rapidly with sulfide, though individual oxides will react with different rates (Pyzik and Sommer, 1981; Canfield, 1989; see below). The importance of iron oxides in supplying iron for early pyrite formation at FOAM comes from the observation that within the top 10 cm, pyrite seems to form directly from the consumption of iron oxides (fig. 1A). Also, the amount of pyrite found at 20 cm depth nearly matches the amount expected from the complete pyritization of the iron oxides associated with suspended sediment collected at FOAM (fig. 1B; see also Canfield, 1989). This is further indication that the iron oxides in depositing sediment are the most important source of pyrite iron.

Although most of the pyrite at FOAM is formed from reaction between sulfide and iron oxides, some continued pyrite formation occurs below the zone of iron oxide depletion. For example, there is a relatively small, but steady, increase in concentration of total reduced sulfur to about 100 cm depth (fig. 1B). Assuming that the mineralogy of the particles depositing at FOAM has remained roughly constant over time, about 0.2 wt percent sulfur is added between 20 and 100 cm depth. Roughly 20 to 25 percent of this increase could come from the dissolution and pyritization of magnetite (see Canfield and Berner, 1987). Most of the increase, however, probably comes from the reaction between sulfide and iron-containing silicate minerals. Some evidence for this comes from a significant increase (approx 0.04 wt percent) in the pyrite sulfur content of the 21 to 63 μm size fraction (fig. 2), reflecting the pyritization of layered silicates.

Below 100 cm, little or no further increase in total sulfur content can be discerned (fig. 1B). There is, however, evidence for continued *slow* reaction between sulfide and iron minerals. This is seen in the gradual increase in the pyrite sulfur content of the 21 to 61 μm size fraction (fig. 2). A similar increase likely occurs in the other size fractions and in the total sediment but is too small to be easily observed.

The increase in pyrite sulfur in the 21 to 63 μm size fraction is of particular interest because sheet silicates contain the largest fraction of unpyritized iron at FOAM, and their rate of reaction controls how quickly complete pyritization of FOAM sediment could occur (see also below). Two very simple models may be constructed to *approximate* the rate of reaction between sheet silicates and sulfide and to estimate the time required for their complete pyritization. In the first model, the rate of reaction is assumed to be independent of iron concentration, and the observed rate of sulfur incorporation into the 21 to 63 μm size fraction continues until iron is completely consumed. Because the data show some scatter we have chosen three starting depths for calculating the rate of sulfur increase: 25, 65, and 105 cm. A least squares linear regression was applied to the data for each of these starting points and the times for the complete pyritization of the remaining 1.8 wt percent Fe (with a sediment deposition rate of 0.09 cm yr^{-1}; Krishnaswami and others, 1984) range between 100,000 to 170,000 yrs (table 3). These results must be considered a minimum time for complete pyritization, because longer times will be required if the rate is proportional to the concentration of unreacted iron (see below), and if the residual iron contained in the silicates becomes less reactive with continued consumption to form pyrite.

We are unable to comment on how the reactivity of silicates might change with continued reaction; this will require the study of more slowly depositing sediments than FOAM, where sulfide contacts iron minerals for longer periods of time. We can, however, address how the reaction rates between iron silicates and sulfide might change if the rate were proportional to the concentration of iron. With this scenario the rate of reaction between sulfide and iron may be defined as:

$$dFe/dt = -akFe \tag{2}$$

where Fe is the concentration of iron (wt percent), k is the reaction rate constant (yr^{-1}), t is time (yr), and "a" is the stoichiometric constant (0.87) necessary to convert pyrite sulfur formation rates (fig. 2) into iron consumption rates. This expression does not include a proportionality with respect to sulfide concentration, though one certainly must exist. The dissolved sulfide concentrations in the zone of silicate pyritization at FOAM are, however, reasonably constant at between about 3 to 6 mM (fig. 1B). Values of k are identical to the reciprocal of the times needed for complete iron sulfidation in table 3, and the half lives ($t_{1/2}$) for iron (table 3) are estimated as:

$$t_{1/2} = \ln(2)/k \tag{3}$$

The data suggest that at FOAM iron will be consumed with a half life of between about 70,000 to 120,000 yrs. In figure 5, extreme values for $t_{1/2}$ of 37,000 and 145,000 yrs are shown to bracket completely the sulfur data from the 21 to 63 μm size fraction.

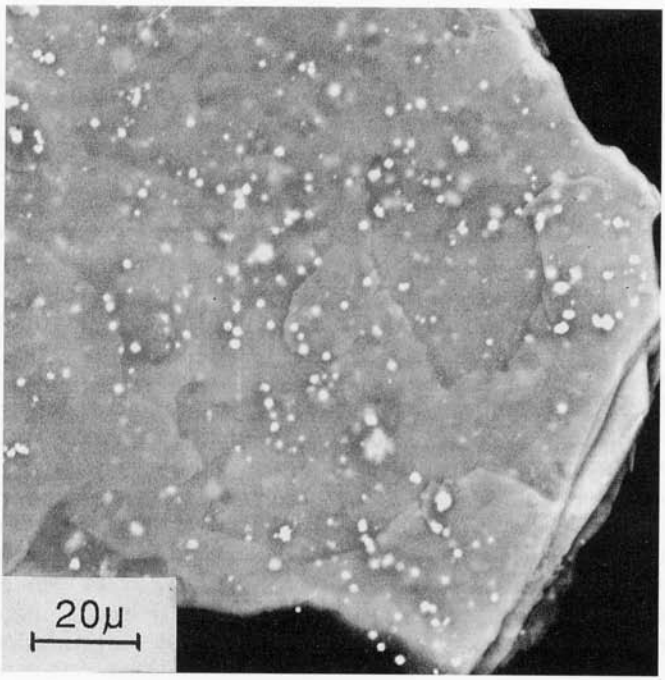

A

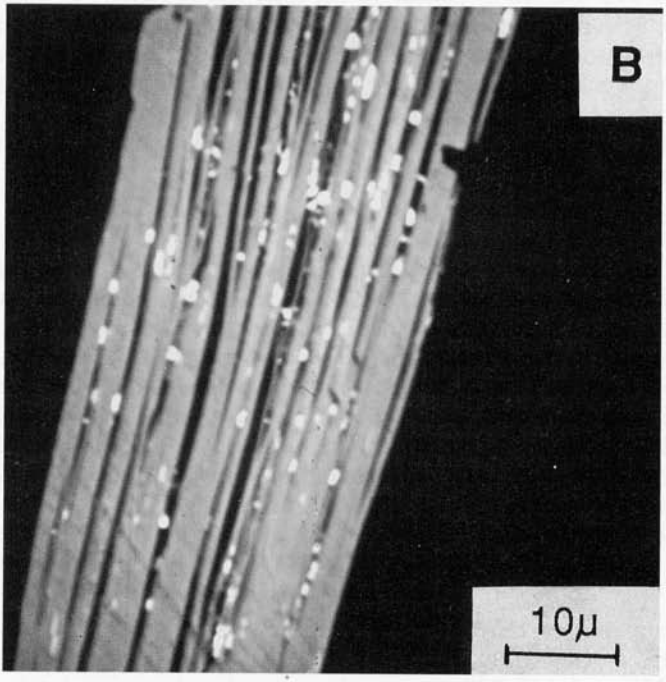

B

Fig. 4(A) SEM photomicrograph of a sheet silicate grain in the 21 to 63 μm size separate from the 210 to 220 cm depth interval at FOAM. An iron sulfide mineral (likely pyrite, verified using EDS and comparing to pyrite standards) is apparent as bright white dots in this backscatter image. (B) Sheet silicate grain from the 250 to 260 cm depth interval, cut in thin section. Again, the bright white dots in this backscatter image are pyrite.

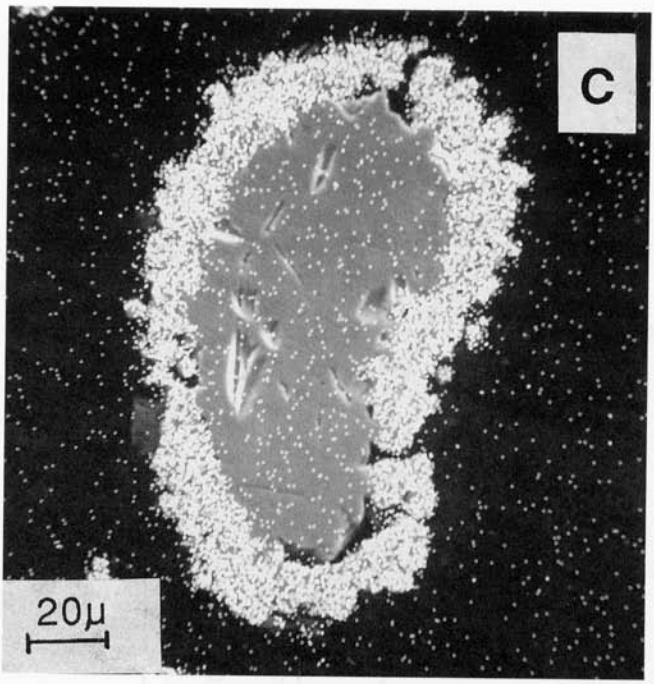

C

(C) EDS sulfur map of pyrite coating magnetite grain (cut in thin section) from 100 to 110 cm depth interval.

A further constraint on reaction rate is given by the total iron data for the 21 to 63 μm size separates (fig. 2). It is conceivable that pyrite does not stay associated with the silicates but becomes detached and forms into framboids of a smaller size; in this way, sulfur data for the 21 to 63 μm fraction may underestimate the reaction rate. However, with framboidal pyrite formation, the concentration of total iron would decrease and not stay constant (as would be expected if no framboidal pyrite was formed). The data (fig. 2) do not show any decrease below 50 cm. The initial

TABLE 3

Reaction rates between H_2S and Fe in 21 to 63 μm size fractions

Starting Depth (cm)	Regression eq.	R^2	Complete Consumption (yr)	$t_{1/2}$ (yr)	$k \times 10^{-6}$ (yr^{-1})
25	$y = 8.14 \times 10^{-2} + 2.02 \times 10^{-4}x$	0.576	114,000	79,000	8.8
65	$y = 9.45 \times 10^{-2} + 1.38 \times 10^{-4}x$	0.417	167,000	116,000	6.0
105	$y = 7.62 \times 10^{-2} + 2.24 \times 10^{-4}x$	0.540	103,000	71,000	9.7

where:
y = wt percent S
x = sediment depth (cm)

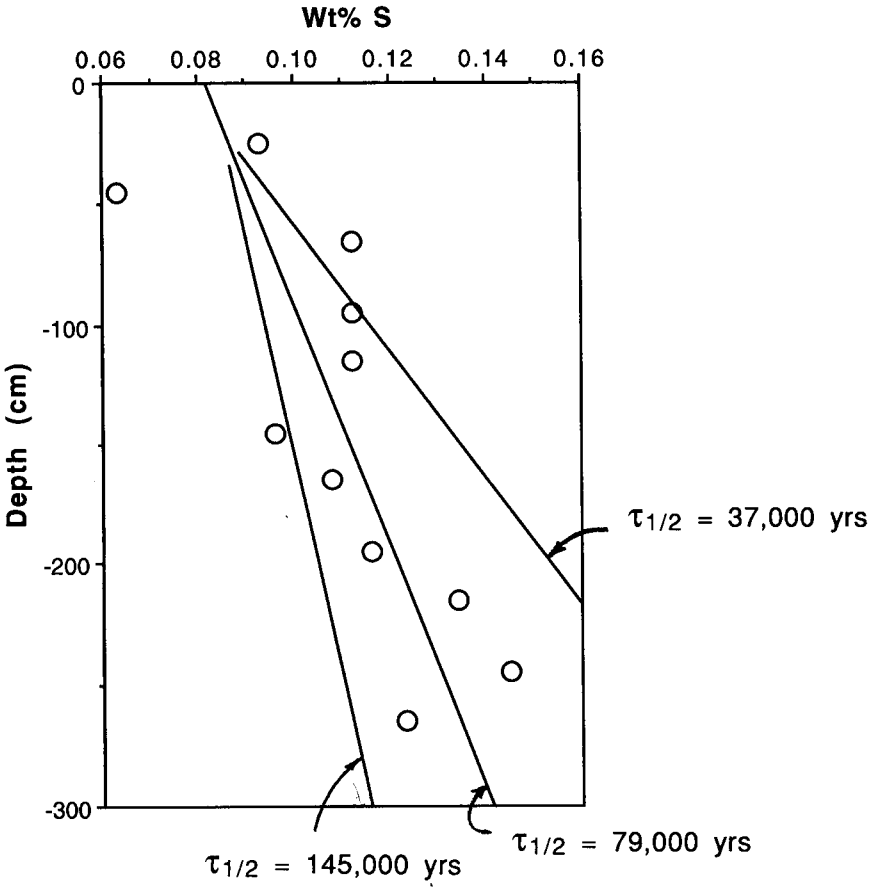

Fig. 5. Lines predicting pyrite sulfur formation rates from iron contained in sheet silicates from the 21 to 63 μm size separates. The different lines represent different formation rates assuming various half-lives for the iron with respect to reaction with sulfide. The "best fit" so the sulfur data assumes a half life for the iron of 79,000 yrs.

decrease between the surface and 50 cm likely reflects the formation of framboidal pyrite from surface coatings of iron oxides. A similar decrease was also observed in the clay fraction (fig. 2).

Sulfur isotopes.—The isotopic composition of sulfur in the different size fractions can be used to test and, in principle, constrain the reaction rates of different iron phases toward sulfide as outlined above. As discussed by many authors, during dissimilatory sulfate reduction, bacteria discriminate in favor of the lighter sulfur isotope (^{32}S) by between about 30 to 60 permil, depending on factors such as sulfate reduction rate and temperature (see for example, Kaplan, Emery, and Rittenberg, 1963; Kaplan and Rittenberg, 1964; Goldhaber and Kaplan, 1980; Chanton, Martens, and Goldhaber, 1987). During continued sulfate depletion

with sediment depth, this fractionation causes the residual sulfate to become progressively enriched in ^{34}S. Hence, the sulfide produced from this residual sulfate also becomes enriched in ^{34}S (Kaplan, Emery, and Rittenberg, 1963; Goldhaber and Kaplan, 1980; Jørgensen, 1979; Chanton, ms). The FOAM site is no exception, as sulfide reaches a $\delta^{34}S$ value of 10.6 permil at depth, which is roughly 40 permil greater than the first formed sulfides near the sediment surface (fig. 3). With this distribution of isotopic values, the earliest formed pyrites should be the lightest isotopically, and the latter formed pyrites heavier.

The data, in fact, support this suggestion. At 4.5 cm depth, all size fractions have nearly the same isotopic composition (approx −30 permil). This similarity likely reflects the early pyritization of iron oxides (with sulfide of the same isotopic composition) associated with each of the different size fractions; for example, the interlayer iron oxides in the 21 to 63 μm fraction as described earlier. With depth and continued pyritization, the 4 to 21 μm size fraction, which contains most of the early formed framboidal pyrite, is always the lightest isotopically. The 21 to 63 μm size fraction, which contains pyrite formed deeper in the sediment, from isotopically heavier sulfide, is enriched in ^{34}S by between 10 to 15 permil over the pyrites in the 4 to 21 μm fraction.

The pyrites in the clay size fraction (<4 μm) have an isotopic composition very similar to those in the 21 to 63 μm fraction. Such a result may be expected if, like the 21 to 63 μm fraction, the iron associated with the clays (mostly silicate iron below 10 cm) reacts slowly with sulfide, and the resulting pyrite stays associated with the clay fraction. Reaction rates are difficult to determine from the sulfur concentration data (fig. 2); however, the reaction between the iron in the clay fraction and sulfide must be slow. In support of this we note that the clay fraction contains, on average, between 35 to 40 percent of the unpyritized iron at FOAM, and still, pyrite forms only very slowly (fig. 1B). From figure 2, sulfur in the clay fraction appears to increase to 100 cm depth, perhaps reflecting the pyritization of clay-iron and retention of these pyrites. The decrease in sulfur concentration below this depth, then, could result from the transformation of fine grained, clay-associated pyrites into larger framboidal pyrite. The small decrease in wt percent clay-iron from 5.18 (90–100 cm) to 4.91 (290–300 cm; data not shown) would be consistent with this hypothesis. The concentration of sulfur, then, would reflect the rate of sulfur reaction with iron, balanced with the formation rate of larger framboidal pyrite; the isotope data would integrate the isotopic compositions of the sulfur added to the clay fraction but not yet converted to a larger grain size.

The pyrite overgrown onto magnetite is the most dynamic of all the different pyrite pools. Its isotopic composition increases by 20 permil with sediment depth and seems to follow reasonably closely the isotopic composition of pore water sulfide. The reason for such a dynamic behavior is, as discussed by Canfield and Berner (1987), that the pyrite rimming magnetite does not aaccumulate but reaches a terminal thickness. In this way, new pyrite is constantly added to the inner part of the

pyrite layer by the reaction between sulfide and magnetite, and older pyrite is shed from the outer part of the layer. The large changes in the isotopic composition of pyrites rimming magnetites demonstrate a relatively short residence time for pyrites in the rim. These results would suggest that after diagenesis is complete, the pyrite covering magnetite will give the isotopic value of the last sulfide remaining before reacting completely from solution.

The isotopic composition of sulfides at FOAM display some other interesting features. Perhaps the most prominent of which is the relatively heavy isotopic values for all sulfides in the 20 to 30 depth interval. This region is unique in FOAM depositional history, as X-radiographs show the sediment to be very well laminated with minimal evidence for bioturbation (Krishnaswami and others, 1984). It appears that a massive depositional event occurred, perhaps due to sediment scouring and redeposition in a large storm, probably over a very short time interval. The results seems to have been the rapid burial of very degradable organic matter without bioturbation, and the formation of pyrite under rather "closed" conditions (see Goldhaber and Kaplan, 1980; Jørgensen, 1979), which quickly reached relatively heavy values. This interpretation is somewhat speculative; however, the strong association between laminated sediment and abnormally ^{34}S enriched pyrites argues for short term non-steady state deposition conditions. This depth interval will not be included in the discussion to follow.

Another feature is a strong increase, with depth, in the $\delta^{34}S$ of pyrite. This enrichment is to be expected with the continued formation of pyrite from ^{34}S enriched sulfide, as discussed above. Finally, a curious feature is the relatively heavy $\delta^{34}S$ of pyrites in the 21 to 63 μm size fraction at the sediment surface. These values likely reflect the isotopic composition of a small amount of detrital pyrite (perhaps from marshes lining the coast, see p. 663 and Canfield, 1989) associated with this size fraction.

To test whether the isotopic data are consistent with the sulfur concentration data presented earlier, the isotopic composition of sulfide in the various size fractions (excluding magnetite) has been predicted. In this calculation, sulfide is added to the preexisting sulfur pool by an amount based on the increase in sulfur concentration (fig. 2) and the average isotopic composition of pore water sulfide in a chosen depth interval. For the clay fraction (<4 μm), the calculation has been made only to 100 cm. No isotopic fractionation has been assumed for the reaction between sulfide and iron. Also, in the absence of more data, the pore water profile of sulfide has been generated by linear extrapolation between the available data. These calculations also assume that the isotopic composition of dissolved sulfide, with depth, has remained constant during the depositional history at FOAM. It is further assumed that the mineralogy of the depositing particles has remained constant over time.

The results (fig. 6) show that the magnitude of change observed in the isotopic composition of sulfur in the different size fractions is similar to that predicted from the combined sulfur concentration–H_2S isotope

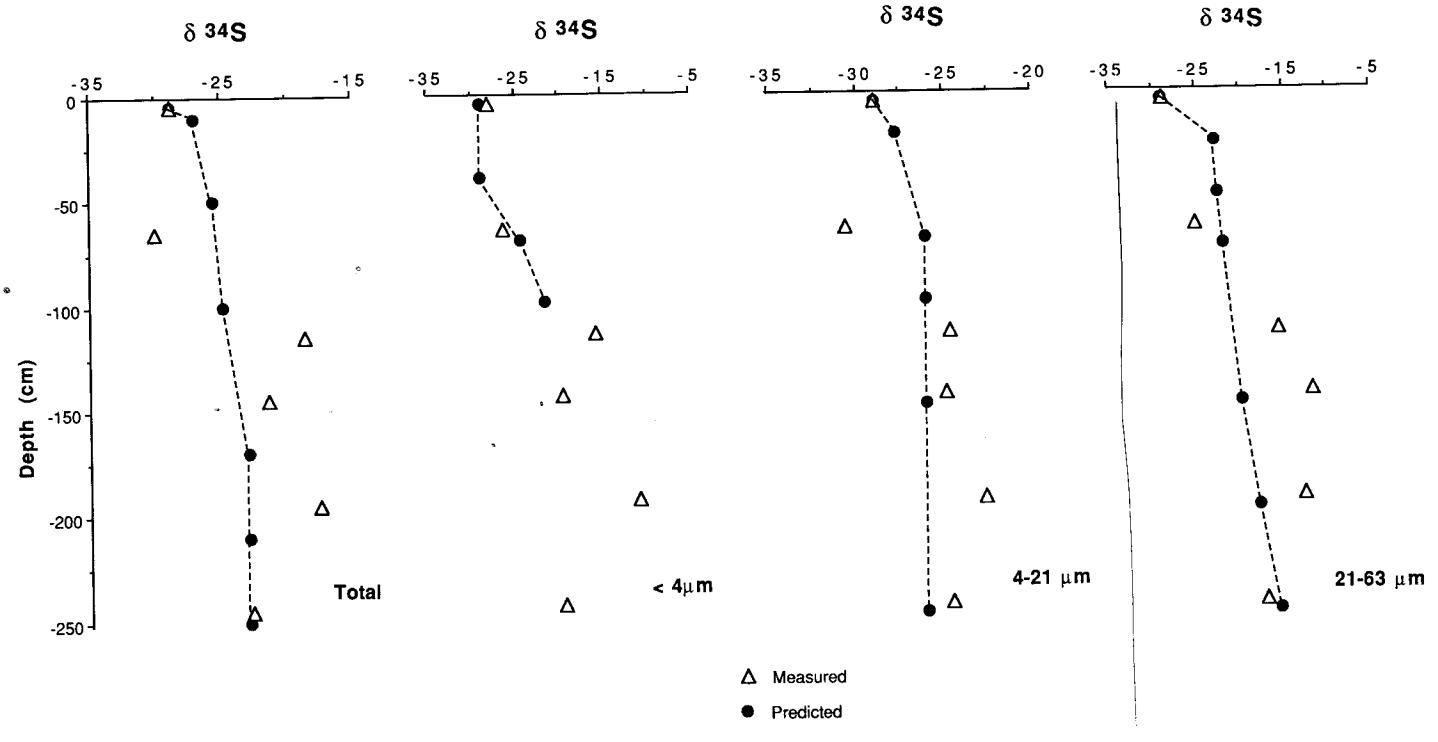

Fig. 6. The isotopic composition of reduced sulfur is predicted for the various size fractions by combining the increases in sulfur concentration with depth (figs. 1B and 2) with the isotopic composition of dissolved sulfide with depth (fig. 3). Predicted values are compared to measured data (see text for details).

data; though in the middle regions of the core (120–200 cm), the predicted values are generally lower than the actual values. Such a mismatch could result from an incomplete or inaccurate knowledge of the $\delta^{34}S$ distribution of dissolved sulfide (see methods) or nonsteady-state conditions, where in the past, the isotopic composition of sulfide was relatively enriched farther up in core than at present. Another possibility is that the isotopic compositions of sulfides formed initially near the sediment surface have been somewhat variable over time (similar to the excursion in the 20–30 cm depth interval, but not as extreme). In general though, the predictions are reasonably close to the data and confirm that sulfur concentration data (figs. 1 and 2) give a good representation of the progressive reaction between sulfide and the various iron mineral phases with depth at FOAM.

DOP and iron limitation.—Our results show that at FOAM, below a depth of about 50 to 100 cm, iron minerals react only very slowly with sulfide, and as a result, sulfide accumulates in the pore water. Berner and Westrich (1985) have shown that with complete retention of the sulfide produced from sulfate reduction, 1.05 wt percent S should be added below 12 cm depth. A roughly 0.2 wt percent increase is seen in figure 1B, which is about 20 percent of the expected value (Berner and Westrich, 1985, show an increase of between 0.25–0.45 wt percent S, but their pyrite values were not reported on a carbonate-free basis). A simple calculation shows that the dissolved sulfide gradient at FOAM (fig. 1B and Canfield and Berner, 1987) will support the diffusional loss of the 80 percent S that is not reacted below 12 cm. Hence, below 12 cm most of the sulfide produced by sulfate reduction does not react with sedimentary iron and is lost from the sediment by diffusion. Yet, relatively low DOP values of about 0.39 to 0.44 (table 2) are observed at all depths below 10 cm. DOP results would indicate that pyrite formation is not iron limited but instead limited by the availability of sulfide. This dichotomy demonstrates a fundamental problem with using DOP to determine iron or sulfide limitation in pyrite formation. The problem is that although DOP can give some measure of the amount of iron that is potentially reactive toward sulfide, it says nothing about the actual reactivity of the iron. So, at FOAM, after iron oxides are reacted to form pyrite, the next reactive iron phases are iron silicates which are consumed only very slowly by reaction with sulfide. The production rates of sulfide are much faster, so that most of the sulfide produced below the zone of iron oxide depletion is lost and not retained in the sediment.

We propose that, independent of DOP calculations, a better measure of whether iron or sulfide limits pyrite formation comes from comparing the reaction rates of sulfide toward iron with rates of sulfide production by sulfate reduction. In this way, when sulfate reduction rates are lower than the rates of reaction between sulfide and iron, pyrite formation is limited by the availability of sulfide. Conversely, when sulfate reduction rates are greater, sulfide will accumulate and diffuse from the sediment pore waters, and pyrite formation is limited by the availability of iron.

To compare the rates of the two processes we have first compiled data on the reaction rates between sulfide and iron. Reaction rates will depend on many factors such as sulfide concentration, the concentration of iron minerals, and the specific surface area of the iron phases. We have chosen a standard dissolved sulfide concentration of 1 mM for the comparison. We recognize that reaction rates may be much slower at lower sulfide concentrations, which characterize the surface zone of sediments (fig. 1B); however, we feel that 1 mM is a good (though somewhat arbitrary) sulfide value by which to separate iron limitation from sulfide limitation. In other words, diffusional loss of sulfide from a sediment should not be so important with dissolved sulfide concentrations of less than 1 mM. Iron reactivity will be expressed as the value k (yr^{-1}) as in eq 2, which is related to the half-life of iron with respect to consumption by sulfide (eq 3).

Iron reactivities are compiled in table 4 in order of decreasing k, with the following explanatory notes. The k value for goethite is from the data of Pyzik and Sommer (1981) assuming a specific surface area of 30 m^2 g^{-1}. Also, Pyzik and Sommer (1981) found that the reaction rate was 100 times faster for a fine grained X-ray amorphous iron oxyhydroxide (specific surface area 133 m^2 g^{-1}), which we have assumed is ferrihydrite. Canfield (1989) found that pure fine grained, synthetic, lepidocrocite (at a concentration of 30 mM Fe, surface area unknown) consumed nearly all an 11 mM sulfide solution in less than 4 hrs. Assuming a square root dependency of reaction rate on sulfide concentration (see Pyzik and Sommer, 1981; Canfield and Berner, 1987) a minimum k value (for a 1 mM sulfide solution) of 85 y^{-1} is calculated. We are unaware of any published studies on the reaction rates between hematite and sulfide. In a simple experiment we added powdered reagent hematite (Merck lot # 8565769, surface area 1.7 m^2 g^{-1}) at a concentration of about 30 mM to three sulfide solutions ranging in concentration between 1 and 3.5 mM. The solutions were buffered at pH 7.5, and we followed the consumption of sulfide over the course of two days. All the consumption data are consistent with a k value of 12 yr^{-1} for 1 mM sulfide.

TABLE 4

Reactivity of Iron Minerals

Iron Mineral	(yr^{-1}) k
Ferrihydrite	2200
Lepidocrocite	>85
Goethite	22
Hematite	12
Magnetite (uncoated)	6.6×10^{-3}
"Reactive" Silicates	3×10^{-3}
Magnetite (coated)	1.3×10^{-3}
Sheet Silicates	8.2×10^{-6}
Ilmenite, Garnets	
Augite, Amphibole	$\ll 8.2 \times 10^{-6}$

The k value for uncovered magnetite is from Canfield and Berner (1987) with a specific surface area of 600 $cm^2\ g^{-1}$ (see Canfield and Berner, 1987, for surface area determination). For covered magnetite we note that the rate of dissolution is slower than for uncovered magnetite (Canfield and Berner, 1987) but fast enough such that large changes are observed in the $\delta^{34}S$ of the pyrite rimming the magnetite (fig. 3). A k value 5 times less than for uncovered magnetite is probably reasonable. The "reactive" iron silicates between 20 and 100 cm depth at FOAM are not well defined (see earlier), but with a concentration of about 0.15 wt percent iron, and complete consumption in about 800 yrs, an approximate value for k can be determined (table 4). As discussed, sheet silicates react rather slowly at FOAM, even at a sulfide concentration of 3 to 6 mM, which is greater than the sulfide level used in our comparison. We will use the k values from table 3, recognizing that they may be lower for a 1 mM sulfide solution. Finally, from SEM observations, the iron-containing mineral phases of ilmenite, augite, various amphiboles, and garnet show no signs of reaction with sulfide at 300 cm depth at FOAM and must have k values even lower than for the sheet silicates.

The values of k for the consumption of organic matter by sulfate reduction (Berner, 1964; Berner, 1980; Westrich and Berner, 1984), may be related to the rate of sulfate reduction by an expression similar to eq 2. Since the concentrations of organic matter in marine sediments are of the same order of magnitude as iron concentrations, a comparison of k values approximates a comparison between sulfide reaction rates with iron and rates of sulfide production. The rate constant, k, for organic matter oxidation by sulfate reduction decreases with increasing age of the organic matter (Jørgensen, 1978b; Berner, 1980; Westrich and Berner, 1984; Middelburg, 1989), or, with depth in a sediment, and in proceeding from the continental margins to the deep-sea (see Middelburg 1989). A representative range of k values for sulfate reduction in three different sedimentary environments and for fresh organic matter are compared to the iron reactivity k values in figure 7 (data from Toth and Lerman, 1977; Westrich, 1983; Westrich and Berner, 1984; Middelburg, 1989).

The following generalizations can be made, though it is important that the rates of sulfide reaction from solution will be dominated by the most reactive iron phase present. The reaction of sulfide with ferrihydrite and lepidocrocite is so fast that iron limitation cannot occur when these phases are present, even at the fastest rates of sulfate reduction with fresh organic matter. As determined by chemical extraction, ferrihydrite and lepidocrocite are abundant in marine sediments (Canfield, 1989; Canfield and Raiswell, 1991; fig. 1A), and their presence explains why sulfide does not accumulate in the surface zone of sediments, even with rapid rates of sulfate reduction (Canfield and Raiswell, 1991; fig. 1A). Both goethite and hematite should also effectively react sulfide from solution at sulfate reduction rates typical of continental margin sediments, though sulfide could accumulate with the decomposition of fresh organic matter.

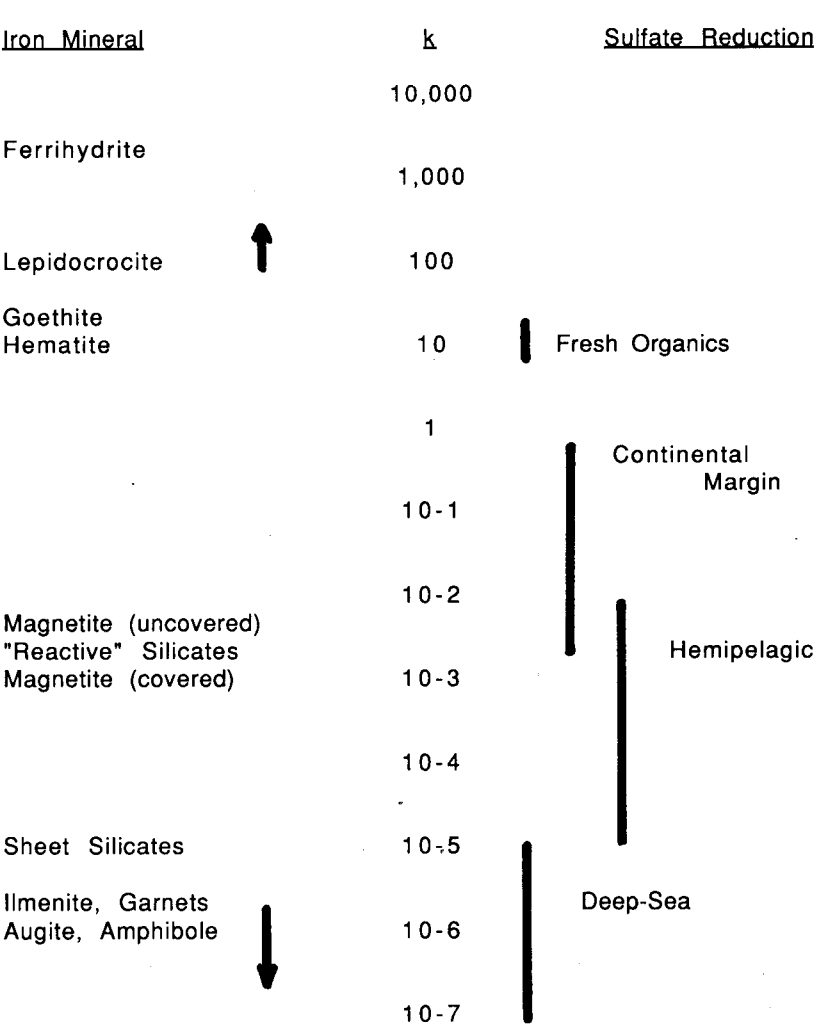

Fig. 7. k values for rates of iron reaction with sulfide are compared to k values for organic carbon decomposition by sulfate reduction for fresh organic matter and for various sedimentary environments. Iron reaction rates are based on a 1 mM sulfide solution (see text for details). Arrows designate phases with k values that may be greater or less than indicated by their place on the graph. When the k for iron reaction with sulfide is greater than the k for sulfate reduction, sulfide is reacted effectively from solution, and pyrite formation is limited by the availability of sulfide. When the k for iron reaction is less than the k for sulfate reduction, sulfide will accumulate, and pyrite formation is limited by the availability of reactive iron. A direct comparison of k's is possible because the concentrations of organic carbon and iron minerals in sediments are of the same order of magnitude (see text).

There is a large decrease in iron mineral reactivity toward sulfide between hematite and the next most reactive iron phases. This explains why the depth where sulfide accumulates in continental margin sediments is so closely related to the depth of iron oxide/oxyhydroxide exhaustion (Canfield and Raiswell, 1991). Also, in continental margin sediments, the availability of reactive iron should limit pyrite formation once the iron oxides are consumed. This is because sulfide will be produced at a rate greater than the remaining iron phases can react it from solution (table 4). In sediments with lower rates of sulfate reduction (such as may be found in some hemipelagic sediments), it is possible that after iron oxides (excluding magnetite) are gone, magnetite and the "reactive" sheet silicates may react sulfide to low levels. In this situation, iron would not limit pyrite formation until after magnetite and "reactive silicates" had become consumed. At this point, even in hemipelagic sediments, sheet silicates would prove to be relatively unreactive toward sulfide (compared to rates of sulfide production), and sulfide would accumulate and not be retained. It is only in slowly depositing deep-sea sediments that the availability of sulfide will surely limit the formation of pyrite. This is doubly true because rates of sulfate reduction in deep-sea sediments are seldom high enough to pyritize completely depositing iron oxides (Canfield and Raiswell, 1991), thus ensuring that these reactive phases will remain to depth. We stress, however, that sulfide does not limit pyrite formation only in deep-sea sediments, but in any sediment where "reactive" iron (compared to rates of sulfide production) persists through the zone of sulfate reduction. An example of such a situation in a continental margin region is the sediments of the Mississippi Delta, where iron oxides are buried below the zone of sulfate reduction (Canfield, 1989).

CONCLUSIONS

Sedimentary iron minerals show a wide range of reactivity toward sulfide; whereas ferrihydrite will be consumed in a 1 mM sulfide solution with a half life of about 4 hrs, the iron in sheet silicates will react with a half life of about 100,000 yrs. Other iron-containing minerals such as ilmenite, garnets, augite, and some amphiboles will take even longer to react. When comparing rates of sulfide reaction with iron to rates of sulfide production by sulfate reduction, it is apparent that in most continental margin sediments, sulfide should not accumulate into solution until after the iron oxyhydroxides and oxides (except magnetite) are consumed in iron sulfide formation. This is consistent with the observation that sulfide does not tend to accumulate in sediments until after iron oxides and oxyhydroxides are, in fact, gone.

The next most reactive iron phases react only very slowly with sulfide—at rates much slower than typical for rates of sulfide production (by sulfate reduction) in continental margin sediments. For this reason, most of the sulfide produced below the zone where iron oxides are consumed will not be retained and will be lost by diffusion. It is clear that

under these circumstances pyrite formation is limited by the availability of reactive iron. Yet, calculated DOP values may be quite low (0.3-0.4), suggesting that the availability of sulfide will limit pyrite formation. We suggest that since DOP cannot resolve the reactivities of unreacted iron toward sulfide, it cannot be used as a reliable indicator of iron or sulfide limitation in the formation of pyrite. DOP, however, may still, under many circumstances, be a useful indicator of paleoenvironments (Raiswell and others, 1988).

Pyrites formed at different stages during diagenesis and from different iron phases have unique sulfur isotopic signatures. For example, the earliest formed framboidal pyrites are up to 40 percent lighter than the pyrites forming much later from magnetite. This is because the later-formed pyrites are formed from sulfide enriched in ^{34}S compared to the earlier pyrites. The depth distribution of $\delta^{34}S$ for pyrites formed at different stages from different iron minerals is consistent with the wide range in rates with which sulfide reacts with iron minerals, as determined independently. Also, it is clear that the final isotopic signal of a sediment will depend critically on the relative amounts of pyrite formed from the rapidly and more slowly reacting iron phases.

ACKNOWLEDGMENTS

This project has evolved and developed over many years. First, we wish to acknowledge the support of R. A. Berner (NSF Grant OCE 8508472) and the help of R. A. Berner, T. Baldwin, K. Ruttenberg, M. Pimer, and A. Goodhue, in collecting the vibracore. DEC wishes to acknowledge the support of the National Research Council (as a NRC postdoctoral fellow) and the kind hospitality of B. B. Jøorgensen and members of his laboratory. RR and SB acknowledge support by the Natural Environment Research Council grant GR3-6254. We wish to acknowledge helpful conversations with B. B. Jøorgensen and B. Thamdrup. This manuscript has benefitted from the careful reviews of J. Leventhal, R. A. Berner, and J. W. Morse.

REFERENCES

Aller, R. C., ms, 1977, The influence of macrobenthos on chemical diagenesis in marine sediments: Ph.D. dissertation, Yale University, New Haven, Connecticut.

———— 1980a, Diagenetic processes near the sediment-water interface of Long Island Sound I. Decomposition and nutrient element geochemistry, *in* Saltzman, B., editor, Estauraine Physics and Chemistry: Studies in Long Island Sound: Advances in Geophysics, v. 22, p. 237–350.

———— 1980b, Diagenetic processes near the sediment-water interface of Long Island Sound II. Fe and Mn, in Saltzman, B., editor, Estuarine Physics and Chemistry: Studies in Long Island Sound: Advances in Geophysics, v. 22, p. 351–415.

Berner, R. A., 1964, An idealized model of dissolved sulfate distribution in recent sediments: Geochimica et Cosmochimica Acta, v. 28, p. 1497–1503.

———— 1970, Sedimentary pyrite formation: American Journal of Science, v. 268, p. 1–23.

———— 1980, Early Diagenesis: A Theoretical Approach: Princeton, New Jersey, Princeton University Press, 241 p.

———— 1984, Sedimentary pyrite formation: an update: Geochimca et Cosmochimica Acta, v. 48, p. 605–615.

Berner, R. A., and Westrich, J. T., 1985, Bioturbation and the early diagenesis of carbon and sulfur: American Journal of Science, v. 285, p. 193–206.

Canfield, D. E., ms, 1988, Sulfate reduction and the diagenesis of iron in anoxic marine sediments: Ph.D. thesis, Yale University, New Haven, Connecticut.

———— 1989, Reactive iron in marine sediments: Geochimica et Cosmochimica Acta, v. 53, p. 619–632.

———— in press, Organic matter oxidation in marine sediments, *in* Wollast, R., Chou, L. and Mackenzie, W. editors, Interactions of C,N,P and S Biogeochemical Cycles NATO-ARW: New York, Springer-Verlag.

Canfield, D. E., and Berner, R. A., 1987, Dissolution and pyritization of magnetite in anoxic marine sediments: Geochimica et Cosmochimica Acta, v. 51, p. 645–659.

Canfield, D. E., and Raiswell, R., 1991, Pyrite formation and fossil preservation, *in* Allison, P. A., and Briggs, D. E. G., editors, Taphonomy: Releasing the Data Locked in the Fossil Record: New York, Plenum Press, p. 337–387.

Canfield, D. E., Raiswell, R., Westrich, J. T., Reaves, C. M., and Berner, R. A., 1986, The use of chromium reduction in the analysis of reduced inorganic sulfur in sediments and shales: Chemical Geology, v. 54, 149–155.

Chanton, J. P., ms, 1985, Sulfur mass balance and isotope fractionation in an anoxic marine sediment: Ph.D. dissertation, University of North Carolina, Chapel Hill.

Chanton, J. P., Martens, C. S., and Goldhaber, M. B., 1987, Biogeochemical cycling in an organic-rich coastal marine basin. 8. A sulfur isotope budget balanced by differential diffusion across the sediment-water interface: Geochimica et Cosmochimica Acta, v. 51, p. 1187–1200.

Dean, W. E., and Arthur, M. A., 1989, Iron-sulfur,-carbon relationships in organic carbon-rich sequences I Cretaceous western interior seaway: American Journal of Science, v. 289, p. 708–743.

Goldhaber, M. B., Aller, R. C., Cochran, J. K., Rosenfeld, J. K., Martens, C. S., and Berner, R. A., 1977, Sulfate reduction, diffusion and bioturbation in Long Island Sound sediments: report of the FOAM group, American Journal of Science: v. 277, p. 193–237.

Goldhaber, M. B. and Kaplan, I. R., 1980, Mechanisms of sulfur incorporation and isotopic fractionation during early diagenesis in sediments of the Gulf of California: Marine Chemistry, v. 9, p. 95–143.

Jørgensen, B. B., 1977, The sulfur cycle of a coastal marine sediment (Limfjorden, Denmark): Limnology and Oceanography, v. 22, p. 814–832.

———— 1978a, A comparison of methods for the quantification of bacterial sulfate reduction in coastal marine sediments. III Estimation from chemical and bacteriological field data: Geomicrobiology Journal, v. 1, p. 49–64.

———— 1978b, A comparison of methods for the quantification of bacterial sulfate reduction in coastal marine sediments. II Calculation from mathematical models: Geomicrobiology Journal, v. 1, p. 29–47.

———— 1979, A theoretical model of the stable sulfur isotope distribution of marine sediments: Geochimica et Cosmochimica Acta, v. 43, p. 363–374.

Kaplan, I. R., Emery, K. O., and Rittenberg, S. C., 1963, The distribution and isotopic abundance of sulfur in recent sediment off Southern California: Geochimica et Cosmochimica Acta, v. 27, p. 297–331.

Kaplan, I. R., and Rittenberg, S. C., 1964, Microbiological fractionation of sulfur isotopes: Journal of General Microbiology, v. 34, p. 195–212.

Krishnaswami, S., Monaghan, M. C., Westrich, J. T., and Turekian, K. K., 1984, Chronologies of sedimentary processes in sediments of the FOAM site, Long Island Sound, Connecticut: American Journal of Science, v. 284, p. 706–733.

Krom, M., and Berner, R. A., 1983, A rapid method for the determination of organic and carbonate carbon in geological samples: Journal of Sedimentary Petrology, v. 53, p. 660–663.

Middelburg, J. J., 1989, A simple rate model for organic matter decomposition in marine sediments: Geochimica et Cosmochimica Acta: v. 53, p. 1577–1581.

Pyzik, A. J., and Sommer, S. E., 1981, Sedimentary iron monosulfides: kinetics and mechanisms of formation: Geochimica et Cosmochimica Acta, v. 45, p. 687–698.

Raiswell, R., and Berner, R. A., 1985, Pyrite formation in euxinic and semieuxinic sediments: American Journal of Science, v. 285, p. 710–724.

Raiswell, R., Buckley, F., Berner, R. A., and Anderson, T. F., 1988, Degree of pyritization of iron as a paleoenvironmental indicator of bottom water oxygenation: Journal of Sedimentary Petrology, v. 58, p. 812–819.

Robinson, B. W., and Kusakabe, M., 1975, Quantitative preparation of sulfur dioxide for 32S/34S analysis by combustions with cuprous oxide: Analytical Chemistry, v. 47, 1179–1181.

Toth, D. J., and Lerman, A., 1977, Organic matter reactivity and sedimentation rates in the ocean: American Journal of Science, v. 277, p. 265–285.

Westrich, J. T., ms, 1983, The consequences and controls of bacterial sulfate reduction in marine sediments: Ph.D. dissertation, Yale University.

Westrich, J. T., and Berner, R. A., 1984, The role of sedimentary organic matter in bacterial sulfate reduction: the G model tested: Limnology and Oceanography, v. 29, p. 236–249.